Contribution from the Department of Chemistry,
University of Rochester, Rochester, New York 14627

The Rhodium(I) Anion Carbonyl(maleonitriledithiolato)(triethylphosphine)rhodate(I) and Acyl Complexes Derived from Its Reaction with Alkyl Halides

CHIEN-HONG CHENG and RICHARD EISENBERG*

Received October 23, 1978

The Rh(I) complex $[Rh(CO)(PEt_3)(mnt)]^-$ generated in situ by the addition of PEt_3 to $[Rh(CO)_2(mnt)]^-$ reacts with various alkyl halides R–X (X = I, R = Me, Et, *n*-Pr, *n*-Bu, *n*-$C_{10}H_{21}$, *i*-Pr, *i*-Bu; X = Br, R = Et, *n*-Pr, *n*-Bu, Bz, allyl, propargyl; X = Cl, R = allyl) in the presence of excess phosphine to form a series of stable neutral Rh(III) acyl species of formula $Rh(COR)(PEt_3)_2(mnt)$. These complexes have been characterized by IR and ^1H NMR spectroscopy, and the structure of a representative member of the series (R = *n*-Pr) has been determined by single-crystal X-ray diffraction methods. The structure determination of $Rh(CO\text{-}n\text{-}Pr)(PEt_3)_2(mnt)$ shows that the complex crystallizes in space group D_{2h}^{15}-*Pbca* in a cell of dimensions a = 20.47 (4) Å, b = 13.61 (3) Å, and c = 18.44 (4) Å with eight molecules per unit cell (ρ_{exptl} = 1.40 (2) g/cm^3; ρ_{calcd} = 1.421 g/cm^3). The coordination geometry of the complex is square pyramidal with the butanoyl group occupying the apical position at a distance of 2.002 (7) Å from the Rh(III) ion. The complex possesses nearly C_s symmetry in the solid state with the triethylphosphine conformations related by a noncrystallographic mirror. The Rh–S and Rh–P bond lengths average 2.320 and 2.348 Å, respectively. In the presence of excess PEt_3, addition of perchloric acid to a solution of $[Rh(CO)(PEt_3)(mnt)]^-$ results in the formation of the rhodium(III) hydride $Rh(H)(CO)(PEt_3)_2(mnt)$. In contrast, the addition of acid to the rhodium(I) complex in acetonitrile in the *presence* of ethylene leads slowly to the formation of an acyl complex which is isolated as $Rh(COEt)(PEt_3)_2(mnt)$ upon adding excess PEt_3.

Introduction

The oxidative addition of alkyl halides to rhodium(I) complexes has been intensively studied since the first report of this reaction in 1964.[1a] However, the majority of the alkyl halides that can be oxidatively added to form stable adducts are limited to "active" ones such as methyl iodide, allyl halides, and benzyl halides.[1] To date, only a few examples of isolable adducts from the reaction of primary alkyl halides RX (R = Et, *n*-Pr, etc., and X = I, Br) with Rh(I) complexes have been reported.[2,3]

In one of these reports,[3] we observed that the Rh(I) complex $[Rh(CO)(PPh_3)(mnt)]^-$, where mnt = maleonitriledithiolate, is reactive toward a series of primary alkyl iodides, leading to the formation of stable rhodium(III) acyl complexes of formula $[Rh(COR)I(PPh_3)(mnt)]^-$. The dithiolate ligand as well as the complex charge clearly activates the Rh(I) ion to react with these substrates. The product acyl complexes were shown to adopt a square-pyramidal geometry by X-ray structural methods, and from NMR studies, it was established that the rhodium position is one of chirality and that the chiral integrity is maintained in solution.

In this paper, we describe the results of an investigation on an apparently more reactive system $[Rh(CO)(PEt_3)(mnt)]^-$. The enhanced reactivity of this anion is evidenced by its ability to react with primary alkyl bromides, which are unreactive with the previously reported triphenylphosphine complex $[Rh(CO)(PPh_3)(mnt)]^-$ and other Rh(I) complexes as well. The synthesis and characterization of a series of neutral acyl complexes obtained from the addition of alkyl halides to $[Rh(CO)(PEt_3)(mnt)]^-$ in the presence of excess PEt_3 and the X-ray structure determination of a representative member of this series are reported. Moreover, the formation of a rhodium(III) hydride and the formation of an acyl complex from ethylene and $[Rh(CO)(PEt_3)(mnt)]^-$ in acid solution are also described. A preliminary communication of this work has appeared.[4]

Experimental Section

All reactions were carried out under a nitrogen atmosphere by using modified Schlenk techniques. Infrared spectra were measured on a Perkin-Elmer Model 467 spectrophotometer and ^1H NMR spectra were recorded on a JEOL MH-100 NMR spectrometer. Elemental analyses were performed by Galbraith Laboratories, Inc., Knoxville, Tenn.

Rhodium trichloride hydrate (Matthey Bishop), tetraphenylarsonium chloride, tetraphenylphosphonium chloride (Ventron), triethylphosphine (Strem), alkyl halides, and tetra-*n*-butylammonium chloride (Eastman) were used as purchased. All solvents were of reagent grade and were dried and degassed before use. The $[Rh(CO)_2(mnt)]^-$ anion was synthesized according to the procedure reported previously.[3]

Preparation of Carbonyl(maleonitriledithiolato)(triethylphosphine)rhodate (I) Ion, $[Rh(CO)(PEt_3)(mnt)]^-$. Syringe addition of PEt_3 to CH_2Cl_2 solutions of $[Rh(CO)_2(mnt)]^-$ as its $(n\text{-}Bu)_4N^+$, PPh_4^+, or $AsPh_4^+$ salt led immediately to the evolution of CO and the in situ generation of $[Rh(CO)(PEt_3)(mnt)]^-$. While attempts to isolate $[Rh(CO)(PEt_3)(mnt)]^-$ from these solutions did not succeed, a method to obtain the Rh(I) anion without excess PEt_3 was developed by using a different workup. To 1.1 g of $[AsPh_4][Rh(CO)_2(mnt)]$ in 20 mL of CH_2Cl_2 was added 0.35 mL of PEt_3. CO evolution was observed. The solution was then evaporated to near dryness, and the resultant yellow oil was washed with ether several times to remove excess PEt_3. The oil was dried in vacuo for 1 day, leading to a puffy yellow product.

Spectrophotometric Titration of $[Rh(CO)_2(mnt)]^-$ with PEt_3. A total of 1.00 mL of 0.142 M PEt_3 in CH_2Cl_2 was added in 0.10-mL increments to 0.5 mL of a CH_2Cl_2 solution which was 0.102 M in $[(n\text{-}Bu)_4N][Rh(CO)_2(mnt)]$. After each addition of 0.10 mL of PEt_3 solution, the absorbance at 1945 cm^{-1} attributed to the carbonyl stretching frequency of $[Rh(CO)(PEt_3)(mnt)]^-$ was recorded. The absorbances after volume correction vs. the volume of PEt_3 solution added were plotted. The end point obtained from the graph was at 0.38 mL of PEt_3 solution added corresponding to 1.06 PEt_3/Rh complex present.

Preparation of $Rh(COR)(PEt_3)_2(mnt)$ from RI and $[Rh(CO)(PEt_3)(mnt)]^-$ Generated in Situ. Most of the complexes were synthesized in the following way. To 0.2 g of $[(n\text{-}Bu)_4N][Rh(CO)_2(mnt)]$ in 5 mL of THF was added 0.2 mL of PEt_3 and 2 mL of RI. Immediate CO evolution was observed. The solution was then set aside until the reaction was complete, as judged by the disappearance of the carbonyl stretch ν_{CO} at 1945 cm^{-1}. Different alkyl halides and the times required for reaction were as follows: MeI, 20 min; EtI, 30 min; *n*-PrI, 2.5 h; *n*-BuI, 3 h. During the course of the reaction a white precipitate was formed and was filtered off at the end of the reaction The filtrate, after addition of ethanol, was evaporated on a rotary evaporator affording the desired yellow product. Yields were ca. 85%. Analytical data follow.

Acetylbis(triethylphosphine)(maleonitriledithiolato)rhodium(III), $Rh(COMe)(PEt_3)_2(mnt)$. Anal. Calcd for $C_{18}H_{33}N_2OP_2S_2Rh$: C, 41.38; H, 6.37; N, 5.36. Found: C, 41.51; H, 6.48; N, 5.34.

Propanoylbis(triethylphosphine)(maleonitriledithiolato)rhodium(III), $Rh(COEt)(PEt_3)_2(mnt)$. Anal. Calcd for $C_{19}H_{35}N_2OP_2S_2Rh$: C, 42.54; H, 6.58; N, 5.22; P, 11.55. Found: C, 43.16; H, 6.45; N, 5.02; P, 11.75.

Butanoylbis(triethylphosphine)(maleonitriledithiolato)rhodium(III), $Rh(CO\text{-}n\text{-}Pr)(PEt_3)_2(mnt)$. Anal. Calcd for $C_{20}H_{37}N_2OP_2S_2Rh$: C, 43.64; H, 6.77; N, 5.09; P, 11.25. Found: C, 43.76; H, 6.90; N, 5.13; P, 11.28.

0020-1669/79/1318-1418$01.00/0

Pentanoylbis(triethylphosphine)(maleonitriledithiolato)rhodium(III), Rh(CO-*n*-Bu)$(PEt_3)_2$(mnt). Anal. Calcd for $C_{21}H_{39}N_2OP_2S_2Rh$: C, 44.68; H, 6.96; N, 4.96; P, 10.97. Found: C, 44.88; H, 7.06; N, 4.90; P, 10.96.

Undecanoylbis(triethylphosphine)(maleonitriledithiolato)rhodium(III), Rh(CO-*n*-$C_{10}H_{21}$)$(PEt_3)_2$(mnt). To 0.20 g of [(*n*-Bu)$_4$N][Rh(CO)$_2$(mnt)] in 5 mL of THF were added 0.2 mL of PEt_3 and 2 mL of *n*-$C_{10}H_{21}I$. The solution was then allowed to react for 18 h. A white precipitate was formed during the reaction and was filtered at the end of the reaction. The filtrate was evaporated on a rotary evaporator to remove most of the solvent. More precipitate was formed and was separated from the solution. After the addition of ethanol, the solution was left at −10 °C overnight affording 0.13 g of yellow crystals (54%). Anal. Calcd for $C_{27}H_{51}N_2OP_2S_2Rh$: C, 49.99; H, 7.93; N, 4.32; P, 9.55. Found: C, 49.84; H, 7.91; N, 4.25; P, 9.34.

3-Methylbutanoylbis(triethylphosphine)(maleonitriledithiolato)rhodium(III), Rh[$COCH_2CH(CH_3)_2$]$(PEt_3)_2$(mnt). To 0.20 g of [(*n*-Bu)$_4$N][Rh(CO)$_2$(mnt)] in 5 mL of THF were added 0.20 mL of PEt_3 and 2.0 mL of isobutyl iodide. The solution was heated at 75 °C for 4 h. The solution was separated from the white precipitate which formed during the course of reaction and was concentrated on a rotary evaporator. Upon addition of ethanol to the solution, 0.16 g of yellow crystals (77%) was obtained. Anal. Calcd for $C_{21}H_{39}N_2P_2S_2Rh$: C, 44.68; H, 6.96; N, 4.96; P, 10.97. Found: C, 44.53; H, 7.09; N, 4.86; P, 11.05.

2-Methylpropanoylbis(triethylphosphine)(maleonitriledithiolato)rhodium(III), Rh($COCH(CH_3)CH_3$)$(PEt_3)_2$(mnt). To 0.50 g of [(*n*-Bu)$_4$N][Rh(CO)$_2$(mnt)] in 15 mL of glyme were added 0.8 mL of PEt_3 and 4 mL of isopropyl iodide. The solution was heated at 77 °C for 4.5 h. The white precipitate formed was filtered, and the filtrate, on addition of ethanol, was concentrated on a rotary evaporator affording a yellow crystalline product. Recrystallization from THF–ethanol yielded 0.11 g (22%) of pure complex. Attempts to improve the yield including longer reaction time did not succeed. Anal. Calcd for $C_{20}H_{37}N_2OP_2S_2Rh$: C, 43.64; H, 6.77; N, 5.09; P, 11.25. Found: C, 43.45; H, 7.23; N, 5.13; P, 11.32.

Preparation of Rh(COR)$(PEt_3)_2$(mnt) from RBr and $[Rh(CO)(PEt_3)(mnt)]^-$ Generated in situ. Two milliliters of RBr (R = allyl, benzyl, propargyl) was added to $[Rh(CO)(PEt_3)(mnt)]^-$ generated in situ by mixing 0.2 g of [(*n*-Bu)$_4$N][Rh(CO)$_2$(mnt)] in 10 mL of THF with 0.2 mL of PEt_3. The solution was allowed to react for 30 min. At the end of the reaction, the precipitate which formed was filtered and washed with THF to dissolve the yellow crystals in it. The THF washings were combined with the filtrate. Addition of ethanol followed by evaporation on a rotary evaporator yielded the desired yellow product. Yields and analytical data follow.

3-Butenoylbis(triethylphosphine)(maleonitriledithiolato)rhodium(III), Rh(COC_3H_5)$(PEt_3)_2$(mnt). Yield 84%. Anal. Calcd for $C_{20}H_{35}N_2OP_2S_2Rh$: C, 43.80; H, 6.43; N, 5.11; P, 11.29. Found: C, 43.55; H, 6.60; N, 4.97; P, 11.22.

Phenylacetylbis(triethylphosphine)(maleonitriledithiolato)rhodium(III), Rh($COCH_2Ph$)$(PEt_3)_2$(mnt). Yield 86%. Calcd for $C_{24}H_{37}N_2OP_2S_2Rh$: C, 48.16; H, 6.23; N, 4.68; P, 10.35. Found: C, 48.15; H, 6.34; N, 4.63; P, 10.36.

3-Butynoylbis(triethylphosphine)(maleonitriledithiolato)rhodium(III), Rh(COC_3H_3)$(PEt_3)_2$(mnt). Yield 33%. Calcd for $C_{20}H_{33}N_2OP_2S_2Rh$: C, 43.96; H, 6.09; N, 5.13; P, 11.34. Found: C, 43.75; H, 6.34; N, 5.06; P, 11.42.

Pentanoylbis(triethylphosphine)(maleonitriledithiolato)rhodium(III), Rh(CO-*n*-Bu)$(PEt_3)_2$(mnt). Two milliliters of *n*-butyl bromide was added to $[Rh(CO)(PEt_3)(mnt)]^-$ generated by the addition of 0.2 mL of PEt_3 to 0.20 g of [(*n*-Bu)$_4$N][Rh(CO)$_2$(mnt)] in 5 mL of THF. The solution was then heated at 60 °C for 16 h. The white precipitate formed was filtered, and the filtrate, after addition of ethanol, was concentrated on a rotary evaporator to a volume of ca. 3 mL, which after being stored at −10 °C yielded 0.13 g of yellow crystalline product (62%). The product was identical with the complex obtained by using *n*-BuI (vide supra) as the substrate, as shown by NMR and IR data.

Butanoylbis(triethylphosphine)(maleonitriledithiolato)rhodium(III), Rh(CO-*n*-Pr)$(PEt_3)_2$(mnt). Two milliliters of *n*-propyl bromide was added to $[Rh(CO)(PEt_3)(mnt)]^-$ generated by the addition of 0.2 mL of PEt_3 to 0.25 g of [(*n*-Bu)$_4$N][Rh(CO)$_2$(mnt)] in 5 mL of THF. The solution was then heated at 60 °C for 16 h. The white precipitate formed was filtered, and the filtrate, after addition of ethanol, was concentrated on a rotary evaporator to afford 0.10 g of yellow crystals (39%). The product is shown to be the same as Rh(CO-*n*-Pr)$(PEt_3)_2$(mnt) formed from $[Rh(CO)(PEt_3)(mnt)]^-$ and *n*-PrI (vide supra).

Propanoylbis(triethylphosphine)(maleonitriledithiolato)rhodium(III), Rh(COEt)$(PEt_3)_2$(mnt). Two milliliters of ethyl bromide was added to $[Rh(CO)(PEt_3)(mnt)]^-$ generated in situ by the addition of 0.3 mL of PEt_3 to 0.25 g of [(*n*-Bu)$_4$N][Rh(CO)$_2$(mnt)] in 5 mL of THF. The solution was then heated at 37 °C for 14 h. Another 1 mL of EtBr and 0.2 mL of PEt_3 were then added and the solution was heated for 10 h more. The white precipitate formed was separated from the filtrate, which after addition of ethanol, was concentrated on a rotary evaporator affording 0.17 g of yellow crystalline product (69%). This product was identical with the corresponding complex obtained from EtI and the Rh(I) anion.

Preparation of Rh(COC_3H_5)$(PEt_3)_2$(mnt) from Allyl Chloride and $[Rh(CO)(PEt_3)(mnt)]^-$ Generated in Situ. One milliliter of allyl chloride was added to $[Rh(CO)(PEt_3)(mnt)]^-$ generated by the addition of 0.2 mL of PEt_3 to 0.20 g of [(*n*-Bu)$_4$N][Rh(CO)$_2$(mnt)] in 5 mL of THF. The solution was left at room temperature for 4 h. The white precipitate formed was filtered and washed with THF. The washings were combined with the filtrate. Addition of ethanol followed by evaporation on a rotary evaporator yielded 0.17 g of yellow crystals (84%). This product was identical with the corresponding product from allyl bromide and the Rh(I) anion.

Preparation of Hydrido(carbonyl)bis(triethylphosphine)(maleonitriledithiolato)rhodium(III), RhH(CO)$(PEt_3)_2$(mnt). Four drops (ca. 0.1 mL) of perchloric acid (70%) were added to $[Rh(CO)(PEt_3)(mnt)]^-$ generated in situ by the addition of 0.3 mL of PEt_3 to 0.30 g of $(AsPh_4)[Rh(CO)_2(mnt)]$ in 10 mL of THF. The precipitate which formed during the reaction was separated from the solution. After the addition of ethanol, the solution was evaporated by vacuum to afford 0.18 g of orange crystals (81%). Anal. Calcd for $C_{17}H_{31}N_2OP_2S_2Rh$: C, 40.16; H, 6.15; N, 5.51; P, 12.18. Found: C, 40.57; H, 6.41; N, 5.45; P, 12.49.

Preparation of Rh(COEt)$(PEt_3)_2$(mnt) from Ethylene and $[Rh(CO)(PEt_3)(nmt)]^-$. $(PPh_3CH_3)[Rh(CO)(PEt_3)(mnt)]$ (0.3 g) was dissolved in 10 mL of acetonitrile and then placed under 1 atm pressure of ethylene. After the addition of 8 drops (ca. 0.2 mL) of perchloric acid (70%), the solution was stirred for 1 day. Upon addition of 0.2 mL of PEt_3 and 20 mL of ethanol, the solution was evaporated on a rotary evaporator affording a brown precipitate. The precipitate was collected and redissolved in THF. The undissolved material was filtered off, and the filtrate, after addition of ethanol, was evaporated slowly to yield 0.070 g of product (29%) which was shown by NMR and IR data to be identical with Rh(COEt)$(PEt_3)_2$(mnt) prepared by other methods (vide supra).

Crystal Structure of Butanoylbis(triethylphosphine)(maleonitriledithiolato)rhodium(III). Data Collection and Reduction. Orange crystals of Rh(CO-*n*-Pr)$(PEt_3)_2$(mnt) suitable for X-ray study were grown from acetone solution at 10 °C. On the basis of precession photographs, it was determined that the crystals belong to the orthorhombic system. The systematic absences were consistent with the space group D_{2h}^{15}-*Pbca*.[5] The lattice parameters were determined at 21 °C from a least-squares refinement of the angular settings of 12 strong high-angle reflections ($(\sin\theta)/\lambda \geq 0.255$)[6] which were centered by using Mo $K\alpha_1$ radiation on a Picker FACS-I diffractometer equipped with a graphite monochromator (λ 0.709 261 Å). The lattice parameters are a = 20.47 (4), b = 13.61 (3), and c = 18.44 (4) Å. An experimental density of 1.40 (2) g/cm^3 determined by the flotation method agrees with a value of 1.42 g/cm^3 calculated for Z = 8.

A crystal of dimensions 0.25 × 0.20 × 0.17 mm mounted along the 210 axis was used for data collection. Intensities were measured by the θ–2θ scan technique. Data were collected at a scan rate of 1°/min with the scan ranging from 0.7° below the $K\alpha_1$ peak to 0.7° above the $K\alpha_2$ peak. Background counts of 10 s duration were measured at each end of the scan. Attenuator foils were automatically inserted when the intensity of the diffracted beam reached 10 000 counts/s. The pulse height analyzer was set for a 90% window centered on Mo $K\bar{\alpha}$ radiation. Data were collected to a maximum 2θ value of 45° from the octant with $h \geq 0$, $k \geq 0$, and $l \geq 0$. Three reflections were monitored every 77 observations. The intensities of the standards did not vary by more than ±3% until near the end of the data collection, when one of the standards started to decrease in intensity sharply due to a slight movement of the crystal position on the diffractometer. An examination after data collection showed the effect

Table I. Final Positional and Thermal Parameters for Rh(CO-*n*-Pr)(PEt_3)$_2$(mnt)

atom[a]	*x*	*y*	*z*	β_{11}[b,c]	β_{22}	β_{33}	β_{12}	β_{13}	β_{23}
Rh	0.410363 (20)[d]	0.28427 (3)	0.318551 (22)	11.80 (13)	33.68 (29)	16.12 (16)	−0.90 (14)	0.18 (10)	0.78 (16)
S1	0.43890 (8)	0.18706 (11)	0.41748 (8)	16.6 (4)	52.3 (10)	22.8 (5)	1.7 (5)	1.0 (4)	8.8 (6)
S2	0.52057 (7)	0.31607 (11)	0.30448 (8)	13.0 (4)	47.7 (9)	22.3 (5)	−1.4 (5)	0.2 (3)	3.4 (5)
P1	0.30564 (8)	0.21441 (12)	0.32613 (9)	14.3 (4)	51.8 (10)	26.0 (6)	−5.9 (5)	1.1 (4)	2.3 (6)
P2	0.39820 (7)	0.35249 (11)	0.20254 (8)	16.2 (4)	38.3 (9)	17.0 (5)	−2.2 (5)	−1.0 (3)	1.1 (5)
C1S2	0.05682 (27)	0.2540 (4)	0.1242 (3)	13.8 (15)	39 (3)	22.1 (19)	2.7 (20)	3.1 (15)	7.4 (22)
C1S1	0.02256 (27)	0.2009 (4)	0.0761 (3)	16.6 (16)	42 (4)	20.0 (19)	2.3 (20)	1.8 (14)	1.7 (22)
C2S2	0.1270 (3)	0.2584 (5)	0.1231 (3)	18.7 (20)	59 (4)	23.0 (21)	1.3 (24)	4.5 (16)	1.5 (24)
C2S1	0.0545 (3)	0.1512 (5)	0.0187 (3)	20.5 (18)	73 (5)	23.0 (22)	6.1 (26)	−0.5 (17)	−3.5 (29)
NS2	0.18253 (27)	0.2619 (5)	0.1252 (3)	17.4 (17)	117 (5)	36.3 (23)	−6.7 (25)	4.7 (16)	−5.7 (29)
NS1	0.0798 (3)	0.3899 (5)	0.4720 (3)	38.5 (23)	123 (6)	33.6 (24)	−18 (3)	4.8 (19)	19 (3)
OAC	0.33466 (21)	0.45512 (29)	0.34932 (22)	22.3 (13)	49.6 (28)	30.4 (15)	12.4 (16)	−5.0 (11)	−7.3 (17)
AC1	0.38083 (29)	0.4086 (4)	0.36652 (29)	17.0 (16)	39 (4)	18.6 (19)	0.7 (21)	1.9 (14)	−2.5 (22)
AC2	0.42618 (29)	0.4407 (5)	0.4268 (3)	23.5 (20)	61 (4)	26.5 (23)	5.9 (23)	−4.1 (16)	−14.6 (27)
C11P2	0.4085 (3)	0.2615 (5)	0.1298 (3)	40.0 (25)	61 (4)	18.1 (20)	−6.8 (29)	−3.9 (18)	−6.4 (25)
C12P2	0.4733 (4)	0.2051 (5)	0.1285 (4)	39.3 (27)	78 (6)	36.7 (28)	32 (3)	−2.5 (22)	−13 (3)
C21P2	0.4591 (3)	0.4436 (5)	0.1781 (3)	21.3 (19)	64 (5)	23.9 (22)	−6.7 (23)	−1.1 (16)	10.2 (26)
C22P2	0.0435 (4)	0.0356 (4)	0.2269 (4)	36.2 (25)	39 (4)	38.5 (27)	16.5 (25)	2.3 (20)	2.5 (27)
C31P2	0.3215 (3)	0.4112 (5)	0.1781 (3)	18.7 (17)	58 (4)	29.3 (22)	4.2 (22)	−4.7 (16)	7.8 (26)
C11P1	0.2854 (3)	0.1600 (6)	0.4129 (4)	17.5 (19)	94 (6)	42.2 (29)	−12.7 (27)	−3.5 (18)	35 (4)
C21P1	0.2343 (3)	0.2889 (5)	0.3059 (4)	13.9 (17)	92 (6)	39.5 (27)	−6.8 (26)	−5.9 (17)	17 (3)
C22P1	0.1667 (3)	0.2413 (7)	0.3230 (4)	14.6 (18)	119 (7)	51 (3)	−16 (3)	−0.7 (20)	21 (4)
C31P1	0.2963 (4)	0.1115 (6)	0.2630 (5)	42 (3)	94 (7)	53 (4)	−45 (4)	7.4 (26)	−13 (4)
C32P2	0.3229 (3)	0.4756 (5)	0.1100 (4)	31.9 (23)	83 (6)	37.5 (29)	2.7 (29)	−8.5 (21)	29 (3)
AC3	0.0977 (4)	0.0279 (5)	0.4701 (4)	34.1 (24)	71 (5)	34.0 (26)	−8.9 (27)	9.4 (20)	−19 (3)
AC4	0.3467 (4)	−0.0008 (6)	0.0204 (5)	46 (3)	109 (7)	51 (4)	−9 (4)	19.8 (28)	15 (4)
C32P1	0.3505 (4)	0.0372 (6)	0.2637 (6)	36.7 (29)	76 (6)	91 (5)	0 (4)	8 (3)	−32 (5)
C12P1	0.2778 (4)	0.2376 (7)	0.4740 (4)	30.2 (25)	150 (8)	28.1 (27)	4 (4)	7.1 (20)	1 (4)

[a] The atom labeling scheme is as follows: C1S*i* is the ethylenic C atom bonded to S*i*; C2S*i* and NS*i* are the nitrile atoms of the dithiolate ligand bonded to C1S*i*; OAC and AC*i* are the acyl oxygen and carbon atoms, respectively; the ethyl C atoms of the PEt_3 ligands are denoted C*ij*P*k* where C*i*1P*k* is the *i*th ethyl group carbon bonded to phosphorus P*k* and C*i*2P*k* is the terminal C atom of that ethyl group. [b] The form of the anisotropic thermal ellipsoid is $\exp[-(\beta_{11}h^2 + \beta_{22}k^2 + \beta_{33}l^2 + 2\beta_{12}hk + 2\beta_{13}hl + 2\beta_{23}kl)]$. [c] Values of the thermal parameters have been multiplied by 10^4. [d] Standard deviations of the least significant figures are given in parentheses.

to be minimal, and, therefore, no correction was made for this deviation. The values of I and $\sigma^2(I)$ were obtained by using the expressions previously described.[7] The value of P used in the expression for the variance was chosen as 0.04.[8] Values of I and σ^2 (I) were converted to F^2 and $\sigma^2(F^2)$ by application of Lorentz and polarization corrections. The linear absorption coefficient for Mo K$\bar{\alpha}$ radiation was sufficiently small (μ = 9.32 cm^{-1}) and no absorption correction was performed. The final data set consisted of 3811 reflections of which the 2614 with $F_o^2 \geq 3\sigma(F_o^2)$ were used in the refinement.

Solution and Refinement of the Structure. The structure was solved by standard heavy-atom methods. A three-dimensional Patterson function map was computed, and from it the position of the Rh atom was determined. Refinement of the positional and isotropic thermal parameters of the Rh atom together with a single scale factor led to discrepancy indices $R = \sum||F_o| - |F_c||/\sum|F_o|$ and $R' = (\sum w(|F_o| - |F_c|)^2/\sum wF_o^2)^{1/2}$ of 0.53 and 0.64, respectively. A succession of difference Fourier syntheses and least-squares refinements revealed the positions of all the remaining nonhydrogen atoms in the structure.[9]

The complete trial structure of 28 nonhydrogen atoms was refined by a least-squares procedure in which the function minimized was $\sum w(|F_o| - |F_c|)^2$ where the weights, w, were taken as $(1/\sigma(F))^2 = 4F_o^2/\sigma^2(F_o^2)$. Only the reflections with $F_o^2 \geq 3\sigma(F_o^2)$ were included in these refinements. Scattering factors for the nonhydrogen atoms were those of Cromer and Mann.[10] Corrections for anomalous dispersion of Rh, P, and S atoms were included in the calculation of F_c using the $\Delta f'$ and $\Delta f''$ values of Cromer and Lieberman.[11] The scattering factor for hydrogen was that of Stewart et al.[12] Two cycles of least-squares refinement with isotropic temperature factors for all the nonhydrogen atoms converged to discrepancy factors R and R' of 0.0571 and 0.0851, respectively. Two more cycles of refinement allowing all nonhydrogen atoms to vary according to an anisotropic thermal model further reduced the discrepancy factors to R = 0.0404 and R' = 0.0591. In the final two cycles of refinement, contributions from the 16 methylene hydrogen atoms were included in F_c on the basis of the idealized parameters d(C–H) = 0.95 Å and H–C–H = 109.5° and fixed isotropic temperature factors of 6.0 Å^2. This refinement led to final convergence at R = 0.0347 and R' = 0.0499 for 253 variables and 2614 reflections with $F_o^2 > 3\sigma(F_o^2)$. The estimated standard deviation of an observation of unit weight was 1.86 e.

Table II. Root-Mean-Square Amplitudes of Vibration (Å)[a]

atom	min	intermed	max
Rh	0.157 (1)	0.166 (1)	0.179 (1)
Ac1	0.170 (10)	0.194 (9)	0.197 (10)
S1	0.179 (2)	0.187 (2)	0.238 (2)
S2	0.165 (2)	0.191 (2)	0.217 (2)
P1	0.163 (3)	0.212 (2)	0.229 (2)
P2	0.169 (3)	0.179 (2)	0.197 (2)
OAc	0.172 (8)	0.209 (6)	0.270 (6)
Ac2	0.178 (10)	0.210 (10)	0.278 (9)
Ac3	0.191 (10)	0.244 (10)	0.317 (10)
Ac4	0.215 (12)	0.332 (11)	0.362 (11)
C1S1	0.177 (9)	0.188 (9)	0.208 (9)
C2S1	0.197 (10)	0.203 (10)	0.267 (9)
NS1	0.203 (10)	0.285 (9)	0.366 (9)
C1S2	0.162 (10)	0.169 (10)	0.222 (9)
C2S2	0.176 (10)	0.218 (9)	0.238 (9)
NS2	0.184 (10)	0.252 (8)	0.335 (8)
C11P1	0.165 (11)	0.203 (10)	0.358 (10)
C21P1	0.162 (11)	0.234 (10)	0.321 (9)
C31P1	0.158 (13)	0.291 (10)	0.397 (11)
C11P2	0.165 (11)	0.243 (9)	0.293 (9)
C21P2	0.185 (10)	0.207 (9)	0.263 (9)
C31P2	0.174 (10)	0.227 (9)	0.251 (9)
C12P1	0.202 (11)	0.266 (10)	0.378 (10)
C22P1	0.158 (12)	0.270 (9)	0.365 (10)
C32P1	0.233 (11)	0.278 (11)	0.418 (12)
C12P2	0.176 (11)	0.250 (10)	0.355 (10)
C22P2	0.162 (11)	0.255 (9)	0.298 (9)
C32P2	0.167 (11)	0.268 (10)	0.332 (10)

[a] Measured along the principal axes of the thermal ellipsoids.

The final difference Fourier map showed peaks near the methyl groups which were ~20% the height of a typical carbon atom in this structure. From their distances to the methyl carbons, we were able to conclude that they were due to methyl hydrogens, but no attempt was made to include them in the calculation or refine them. The parameters from the least-squares refinement having R = 0.0347 are thus taken as the final parameters of the structure and are given in Table I. The root-mean-square amplitudes of vibration of the

Table III. ^1H NMR Data and Carbonyl Stretching Frequencies

complex	chemical shift data (δ)[b,c]					coupling constant data, Hz		
	PEt_3[f]		acyl ligand					
	$-CH_2-$	$-CH_3$	α protons	terminal protons	other resonances, assignment, etc.	$J_{\alpha\beta}$	$J_{\psi\omega}$[d]	ν_{CO}[e]
$[Rh(CO)(PEt_3)(mnt)]^-$[a]	1.86	1.12						1945
$Rh(COMe)(PEt_3)_2(mnt)$	2.03	1.06		2.05 s				1697
$Rh(COEt)(PEt_3)_2(mnt)$	2.03	1.06	2.17 q	0.78 t			7	1740, 1680
$Rh(CO\text{-}n\text{-}Pr)(PEt_3)_2(mnt)$	2.04	1.07	2.30 t	0.72 t	1.33($-CH_2-$)	7	7	1724, 1689
$Rh(CO\text{-}n\text{-}Bu)(PEt_3)_2(mnt)$	2.02	1.06	2.29 t	0.76 t	? $[-(CH_2)_2-]$[h]	7	6	1753, 1721, 1686
$Rh(CO\text{-}n\text{-}(CH_2)_9CH_3)(PEt_3)_2(mnt)$	2.02	1.06	2.28 t	0.85	1.22$[-(CH_2)_8-]$	7	7	1700
$Rh[COCH_2CH(CH_3)_2](PEt_3)_2(mnt)$	2.03	1.06	2.18 d	0.73 d	? (-CH<)[h]	6	7	1721, 1695
$Rh[COCH(CH_3)_2](PEt_3)_2(mnt)$	2.02	1.09	?(-CH<)[h]	0.81 d			7	1729, 1688, 1629
$Rh(COC_3H_5)(PEt_3)_2(mnt)$	2.01	1.05	2.99 d	4.94 m	5.6 m (-CH=)	7		1736, 1686
$Rh(COCH_2Ph)(PEt_3)_2(mnt)$	2.02	1.05	3.57 s		7.1 m (-Ph)			1686, 1736
$Rh(COCH_2CCH)(PEt_3)_2(mnt)$	2.04	1.08	3.10 d	2.19		$^4J_{H-H} = 2.4$		1728, 1672
$Rh(H)(CO)(PEt_3)_2(mnt)$	1.94 m[g]	1.14			9.79 d/t (Rh-H)	$^1J_{Rh-H} = 15$, $^2J_{P-H} = 11$		2045

[a] $AsPh_4^+$ is the counterion. [b] In $CDCl_3$. [c] Key: s = singlet, d = doublet, t = triplet, q = quartet, and m = multiplet. [d] $J_{\psi\omega}$ is the coupling constant between the terminal protons and the adjacent protons. [e] KBr pellet; in cm^{-1}. [f] All the methylene and methyl proton resonances in PEt_3 appear as five-line multiplets except where noted. [g] The splitting pattern is different from those of the other methylene protons. [h] The resonances were not observed because of weak intensity coupled with a complicated splitting pattern or overlapping of the signal with more intense resonances.

anisotropically refined atoms are presented in Table II. A tabulation of the final observed and calculated structure factors for the 2614 reflections is included as supplementary material for the paper.[13]

Results and Discussion

Formation of $[Rh(CO)(PEt_3)(mnt)]^-$. Addition of PEt_3 to solutions of $[Rh(CO)_2(mnt)]^-$ as its $n\text{-}Bu_4N^+$, PPh_4^+, or $AsPh_4^+$ salt leads to the substitution of PEt_3 for one and only one of the carbonyl groups to form $[Rh(CO)(PEt_3)(mnt)]^-$. This monocarbonyl complex persists in solution even with excess phosphine present, as determined by an IR-monitored titration of the dicarbonyl complex with PEt_3 in CH_2Cl_2. This result contrasts with the observation reported by Connelly and McCleverty[14] that both carbonyls of $[Rh(CO)_2(mnt)]^-$ are substituted by PEt_3. While existence of the monocarbonyl complex was firmly established by the titration experiment and the spectroscopic data (see Table III), most attempts to isolate the pure complex by using different cations did not succeed. Therefore, this anion, in most cases, was generated in situ by addition of PEt_3 to solutions of $[Rh(CO)_2(mnt)]^-$ before reaction with substrates. One method of obtaining and isolating the monocarbonyl species without excess phosphine is described in the Experimental Section.

The complex $[Rh(CO)(PEt_3)(mnt)]^-$ appears to be significantly more reactive than the analogous PPh_3 complex with alkyl halide substrates (vide infra), and this may be explained in part by the greater σ-donor ability of PEt_3 relative to PPh_3 and its consequent effect on activating the Rh(I) ion. The value of ν_{CO} in the PEt_3 complex, which is lower than that in the PPh_3 derivative, supports this view.

Reaction between $[Rh(CO)(PET_3)(mnt)]^-$ and RX. $[Rh(CO)(PEt_3)(mnt)]^-$, which is generated in situ, reacts with a variety of alkyl halides RX (for X = I, R = Me, Et, *n*-Pr, *n*-Bu, $n\text{-}C_{10}H_{21}$, *i*-Bu, *i*-Pr; for X = Br, R = Et, *n*-Pr, *n*-Bu, Bz, allyl, propargyl; for X = Cl, R = allyl) to yield acyl complexes which are isolated in the presence of excess PEt_3 as analytically pure products of formula $Rh(COR)(PEt_3)_2(mnt)$. The reactivity of $[Rh(CO)(PEt_3)(mnt)]^-$ thus appears to be greater than that of the PPh_3 analogue which reacts only with alkyl iodides and activated alkyl bromides, and it represents an extension over previously studied rhodium(I) complexes in their reactions with alkyl halides. In the presence of excess PEt_3, both RI and RBr react with the rhodium(I) anion to form the same acyl complex, $Rh(COR)(PEt_3)_2(mnt)$. However, the reaction rate of RBr (R = Et, *n*-Pr, *n*-Bu) with $[Rh(CO)(PEt_3)(mnt)]^-$ is much slower than that of the corresponding RI, and the alkyl bromide reactions were therefore done at elevated temperatures. The complex $[Rh(CO)(PEt_3)(mnt)]^-$ also reacts with *i*-PrI, albeit incompletely, to give the corresponding isobutanoyl complex $[Rh(CO\text{-}i\text{-}Pr)(PEt_3)_2(mnt)]$, of which the NMR spectrum shows a doublet at 0.81 ppm[15] corresponding to the methyl protons. An analogous reaction between 1-methylpropyl iodide and $[Rh(CO)(Pet_3)(mnt)]^-$, however, resulted in the decomposition of the Rh(I) complex to some unknown brown species and did not yield the desired acyl complex.

The formation of $[Rh(COR)(PEt_3)_2(mnt)]$ probably occurs by the sequence shown in Scheme I. This includes oxidative addition of the alkyl halide, alkyl group migration to form the corresponding acyl species, and PEt_3 substitution of the halide ion to form the isolated pentacoordinate bis(phosphine) complex. Evidence in support of the last step in this sequence is obtained when $[Rh(CO)(PEt_3)(mnt)]^-$ is allowed to react with BzBr in the absence of excess PEt_3. This reaction leads to the formation of the anionic phenylacetyl complex $[Rh(COBz)Br(PEt_3)(mnt)]^-$ which exhibits magnetic nonequivalence of the α-methylene protons of the acyl group through an AB quartet centered at δ 4.12 ppm. This species is analogous to the anionic complexes $[Rh(COR)X(PPh_3)(mnt)]^-$ reported previously by us[3] which were found to have diastereotopic α-methylene protons and shown by a structure analysis to have a square-pyramidal geometry with the acyl group in the apical position. Addition of PEt_3 to $[Rh(COBz)Br(PEt_3)(mnt)]^-$ results in rapid conversion of the AB quartet to a singlet at δ 3.57 ppm characteristic of the isolated complex $[Rh(COBz)(PEt_3)_2(mnt)]$.

Scheme I

$$[Rh(CO)(PEt_3)(mnt)]^- + RX \rightarrow$$

$$[Rh(CO)X(R)(PEt_3)(mnt)]^- \xrightarrow{\text{insertion}}$$

$$[Rh(COR)X(PEt_3)(mnt)]^- \xrightarrow{PEt_3} Rh(COR)(PEt_3)_2(mnt)$$

Alternative possibilities to the sequence shown in Scheme I include (1) phosphine substitution for halide prior to the migratory insertion and (2) phosphine addition to $[Rh(CO)(PEt_3)(mnt)]^-$ prior to the reaction with RX as R^+

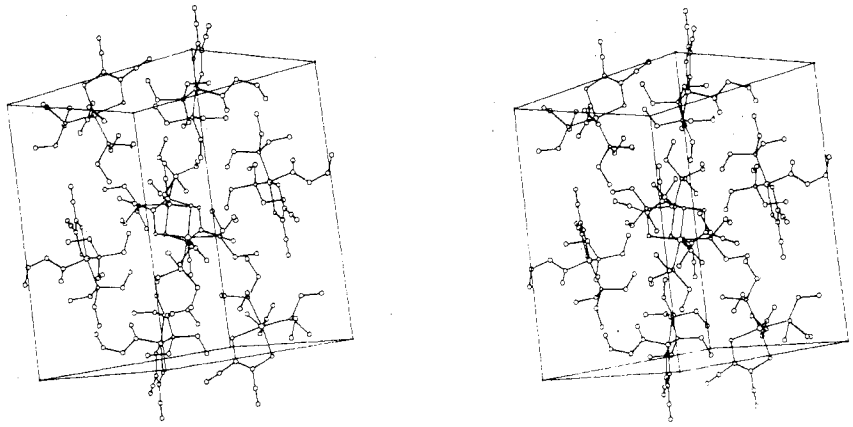

Figure 1. Packing diagram of Rh(CO-*n*-Pr)$(PEt_3)_2$(mnt). The orientation of the unit cell is such that *a* is vertical, *b* + *c* is horizontal, and *c* − *b* is pointing toward the viewer.

followed by migratory insertion to form the acyl. The latter of these possibilities seems remote in view of the fact that the starting Rh(I) complex in the absence of excess phosphine reacts readily with alkyl halides.

The neutral acyl complexes Rh(COR)$(PEt_3)_2$(mnt) are five-coordinate with the acyl group occupying the apical position, as determined from the X-ray structural study (vide infra). Although the structure is similar to that of the anionic complex $[RhX(COR)(PPt_3)(mnt)]^-$, the presence of the two PEt_3 ligands in the basal plane removes the chirality at the Rh center and renders the α-methylene protons equivalent. NMR data and CO stretches of these neutral complexes are summarized in Table III.

In addition to forming the bis(triethylphosphine)–acyl complex, the reaction of RX with $[Rh(CO)(PEt_3)(mnt)]^-$ in THF in the presence of excess PEt_3 yields a white precipitate which is identified as $PEt_3R^+X^-$ and is obtained separately from the reactions of RX with PEt_3.

Reaction of H^+ with $[Rh(CO)(PEt_3)(mnt)]^-$. The reactivity of $[Rh(CO)(PEt_3)(mnt)]^-$ is further demonstrated by hydride formation when acids are added to a THF solution of the complex. With excess PEt_3 present, the addition of $HClO_4$ yields an isolable yellow-orange hydride formulated as RhH(CO)$(PEt_3)_2$(mnt) on the basis of elemental analysis and IR and NMR spectral data. The IR spectrum shows a strong band at 2045 cm^{-1} assigned as ν_{CO} and a medium band at 2000 cm^{-1} assigned as ν_{Rh-H}, and the NMR spectrum exhibits, in addition to the PEt_3 resonances, an upfield hydride resonance which appears as a doublet of triplets at δ −9.79 ($^1J_{Rh-H}$ = 15 Hz; $^2J_{P-H}$ = 11 Hz). This complex is six-coordinate with the two phosphines either cis (**1**) or trans (**2**) to each other. In

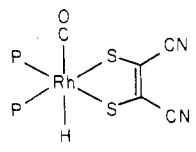

1

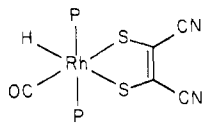

2

both cases the phosphines are equivalent and cis to the hydride in agreement with the splitting pattern of the hydride resonance and cis P–H coupling constants previously reported.[1f,16]

This hydride complex is unstable at room temperature and decomposes to some uncharacterized species even in the solid state, but it seems indefinitely stable at −10 °C. In the absence of excess PEt_3, the addition of $HClO_4$ or *p*-toluenesulfonic acid to yellow solutions of $[Rh(CO)(PEt_3)(mnt)]^-$ yields an immediate red color which rapidly changes to brown indicating complex decomposition.

Rh(COEt)$(PEt_3)_2$(mnt) from Ethylene and $[Rh(CO)(PEt_3)(mnt)]^-$ in Acidic Solution. In the absence of excess PEt_3, addition of $HClO_4$ to a CH_3CN solution of $[Rh(CO)(PEt_3)(mnt)]^-$ under 1 atm of pressure of ethylene results in an immediate color change from yellow to brown followed by slow formation of an acyl species as observed by IR spectroscopy. This acyl species, upon addition of PEt_3, was isolated as Rh(COEt)$(PEt_3)_2$(mnt) identified by ^1H NMR and IR spectroscopy. The reaction probably occurs through several of the well-established steps in the hydroformylation reaction—i.e., hydride formation, olefin coordination, insertion into an M–H bond, and R group migration to give a bound acyl.

Solid-State Structure of Rh(CO-*n*-Pr)$(PEt_3)_2$(mnt). The crystal structure contains discrete monomeric molecules of Rh(CO-*n*-Pr)$(PEt_3)_2$(mnt), as illustrated in Figure 1. The closest intermolecular H···H contacts excluding methyl hydrogens are H1C3P2···H2C3P1 = 2.39, H2AC2···H2AC3 = 2.64, and H2C1P1···H1AC3 = 2.81 Å. (The labeling scheme for the atoms in the structure is given in Table I.) The closest intermolecular hydrogen···nonhydrogen atom contacts are H1C2P1···NS2 = 2.69, H2C3P2···NS2 = 2.71, and H2C3P1···OAC = 2.84 Å. All other intermolecular contacts appear normal and therefore are not tabulated.

The coordination geometry of Rh(CO-*n*-Pr)$(PEt_3)_2$(mnt) is square pyramidal with the butanoyl group occupying the apical position. A stereoscopic view of the complex is shown in Figure 2, and important intramolecular distances and angles are given in Table IV. Although not required crystallographically, the complex possesses essential C_s symmetry with the lone exception of the terminal carbon atom of the butanoyl ligand. The orientation of the acyl group is such that the acyl oxygen points between the two phosphine ligands which in turn exhibit conformations related by the pseudomirror of the complex, as shown in Figure 3.

The structure of Rh(CO-*n*-Pr)$(PEt_3)_2$(mnt) joins a limited number of other Rh(III)–acyl complexes to be structurally characterized by X-ray methods. Of these, the dithiolate anion $[Rh(COEt)I(PPh_3)(mnt)]^-$[3] is most closely related to the present system, and it exhibits a completely analogous structure with the acyl ligand again occupying the apical position of a tetragonal pyramid. The pentacoordination of these two dithiolates contrasts with the distorted octahedral structure in the dimer $Rh_2I_4(\mu\text{-}I)_2(COMe)_2(CO)_2$[19] in which the bridging iodides are trans to the acetyl ligands with a Rh–I bond length 0.322 (3) Å greater than the corresponding terminal Rh–I bond lengths. The well-established tendency of σ-bonded carbon atoms of organic ligands to weaken possible trans ligation can be used to explain both of these observed structure types—i.e., the absence of a sixth ligand in the square-pyramidal structure and elongation of the Rh–I bond trans to acetyl in the iodo-bridged dimer system. Re-

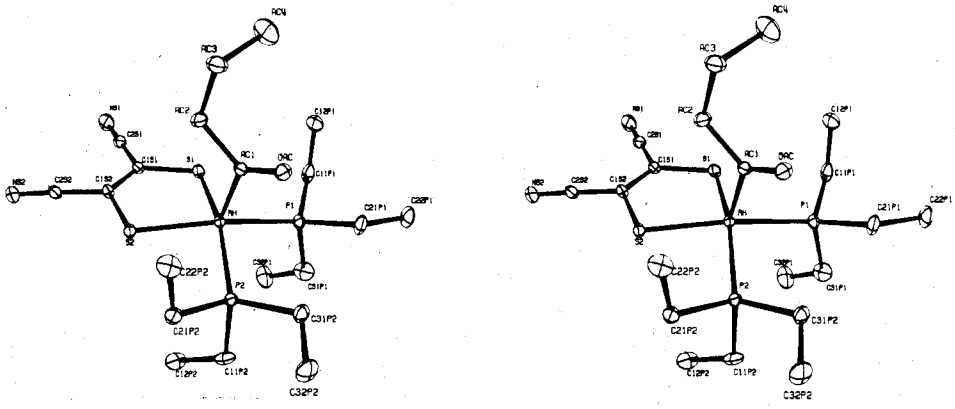

Figure 2. A stereoview of the $Rh(CO\text{-}n\text{-}Pr)(PEt_3)_2(mnt)$ molecule. The thermal ellipsoids correspond to 50% probability distributions.

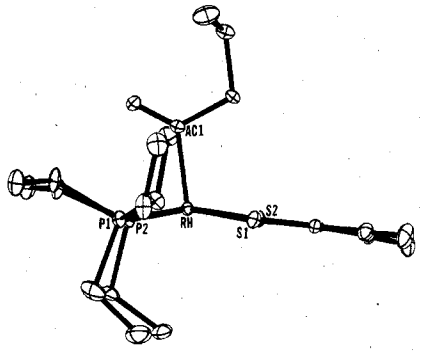

Figure 3. A perspective drawing of the $Rh(CO\text{-}n\text{-}Pr)(PEt_3)_2(mnt)$ molecule. The two triethylphosphines in the complex are in an "eclipsed" conformation relative to each other.

cently two Rh(III)–acyl structures have been mentioned in very preliminary form as part of more extensive studies. Baird and co-workers[17a] have given parameters for the inner-coordination geometry of the complex $RhCl_2(COCH_2CH_2Ph)(PPh_3)_2$ while Stille et al.[17b] have cited bond distances and angles for the complex having one less methylene on the acyl ligand. The results do not agree and further refinement of the structures is essential before the coordination parameters of the complexes can be assessed meaningfully.

In any case, one would expect for a low-spin, pentacoordinate d^6 complex, a square-pyramidal geometry, and that is precisely what is observed here. Moreover, in the well-defined structures, the acyl group is in the unique axial or apical position. This observation contrasts with intuitive thinking about the migratory insertion reaction in which the acyl group should be adjacent to a vacant coordination site and with semiempirical calculations by Hoffmann[18] which for $Mn(COMe)(CO)_4$ suggests that the acyl ligand is preferred in the base of the square pyramid. The low-spin d^6 complex of square-pyramidal geometry would also be expected to have a high barrier to intramolecular rearrangement as this would go through an unfavorable trigonal-bipyramidal intermediate.

In the present structure, the Rh–acyl carbon bond distance is 2.002 (7) Å. This value is in agreement with 2.006 (14) Å found in $[AsPh_4][RhI(COEt)(PPh_3)(mnt)]$[3] and is shorter than Rh(III)–alkyl carbon bond lengths of 2.05–2.26 Å.[19-23] The shortening of the Rh–C bond in these two acyl–dithiolate complexes may be attributed to two factors: (i) the decrease of 0.04 Å in the covalent radius of carbon in going from the sp^3 hybridization of alkyls to the sp^2 hybridization of an acyl[21] and (ii) a back-bonding interaction between a filled d_π orbital of the Rh(III) center and the vacant π^* orbital of the acyl ligand.[3,24] Whatever the importance of the latter interaction, it is interesting to note that the solid-state orientation of the acyl plane defined by C_β–C_α–O_{acyl} in the two dithiolate–acyl complexes is determined solely by steric effects. The C_3 chain

Table IV. Important Intramolecular Distances (Å) and Angles (deg) for $Rh(CO\text{-}n\text{-}Pr)(PEt_3)_2(mnt)$[a]

Rh-Ac1	2.002 (7)	Rh-S1	2.328 (4)
Rh-S2	2.311 (5)	Rh-P1	2.349 (5)
Rh-P2	2.346 (5)	Ac1-OAc	1.181 (7)
Ac1-Ac2	1.514 (8)	Ac2-Ac3	1.509 (9)
Ac3-Ac4	1.513 (11)	S1-C1S1	1.726 (7)
C1S1-C1S2	1.342 (8)	C1S1-C2S1	1.416 (9)
C2S1-NS1	1.152 (8)	S2-C1S2	1.730 (6)
C1S2-C2S2	1.436 (9)	C2S2-NS2	1.140 (8)
P1-C11P1	1.811 (7)	P1-C21P1	1.816 (7)
P1-C31P1	1.829 (9)	P2-C11P2	1.837 (7)
P2-C21P2	1.816 (7)	P2-C31P2	1.819 (7)
C11P1-C12P1	1.553 (11)	C21P1-C22P1	1.560 (9)
C31P1-C32P1	1.503 (11)	C11P2-C12P2	1.531 (9)
C21P2-C22P2	1.540 (9)	C31P2-C32P2	1.532 (9)
Ac1-Rh-S1	102.10 (23)	Ac1-Rh-S2	100.72 (19)
Ac1-Rh-P1	92.31 (21)	Ac1-Rh-P2	92.09 (22)
S1-Rh-S2	87.11 (9)	S1-Rh-P1	87.26 (11)
S1-Rh-P2	165.11 (6)	S2-Rh-P1	166.63 (7)
S2-Rh-P2	85.82 (7)	P1-Rh-P2	96.76 (8)
Rh-Ac1-OAc	125.2 (4)	OAc-Ac1-Ac2	122.1 (5)
Rh-Ac1-Ac2	112.6 (4)	Ac1-Ac2-Ac3	114.7 (5)
Ac2-Ac3-Ac4	112.1 (6)	Rh-S1-C1S1	103.90 (20)
S1-C1S1-C1S2	122.2 (4)	S1-C1S1-C2S1	117.2 (5)
C2S1-C1S1-C1S2	120.6 (6)	C1S1-C2S1-NS1	179.1 (8)
S2-C1S2-C1S1	122.7 (5)	C1S1-C1S2-C2S2	122.4 (5)
S2-C1S2-C2S2	114.8 (5)	C1S2-C2S2-NS2	177.2 (7)
Rh-S2-C1S2	103.99 (22)	Rh-P1-C11P1	115.29 (22)
Rh-P1-C21P1	119.66 (27)	Rh-P1-C31P1	111.58 (26)
C11P1-P1-C21P1	103.1 (3)	C11P1-P1-C31P1	102.9 (4)
C21P1-P1-C31P1	102.3 (4)	Rh-P2-C11P2	112.72 (28)
Rh-P2-C21P2	115.12 (20)	Rh-P2-C31P2	119.43 (21)
C11P2-P2-C21P2	101.6 (3)	C11P2-P2-C31P2	102.4 (3)
C21P2-P2-C31P2	103.3 (3)	P1-C11P1-C12P1	112.6 (5)
P1-C21P1-C22P1	116.0 (5)	P1-C31P1-C32P1	115.6 (6)
P2-C11P2-C12P2	116.7 (5)	P2-C21P2-C22P2	112.7 (4)
P2-C31P2-C32P2	115.9 (5)		

[a] Errors are calculated using the full variance-covariance matrix.

of the acyl ligand in the present structure is oriented toward the dithiolate side of the complex and away from the bulkier phosphine ligands (see Figure 2), while in $[RhI(COEt)(PPh_3)(mnt)]^-$ the acyl plane is oriented differently by 90° such that the ethyl group points between the iodide and one sulfur of the dithiolate, with the sterically smaller acyl oxygen between the PPh_3 ligand and the other dithiolate sulfur.

Other parameters within the structure are more or less as expected. The Rh–S bond lengths of 2.311 (5) and 2.328 (4) Å agree with other Rh(III)–S distances as, for example, 2.333 and 2.316 (3) Å in $Rh(sacsac)_3$,[25] 2.322 (3) and 2.369 (3) Å in $Rh(MeSCH_2CH_2S)_3$,[26] and 2.323 (3) and 2.269 (3) Å in the closely related anion $[RhI(COEt)(PPh_3)(mnt)]^-$[3] (the latter value in this structure which *is* significantly shorter is *trans* to iodide). The Rh–P bond lengths average 2.348 (5) Å and agree with typical Rh(III)–phosphine values reported

elsewhere such as 2.324 (3) Å in $[RhI(COEt)(PPh_3)(mnt)]^-$ and 2.368 (3) and 2.372 (3) Å in $RhCl_3(PEt_3)_2(CHNMe_2)$.[27]

The bond angles about Rh show small deviations from true tetragonal-pyramidal symmetry which can be ascribed to steric effects of the coordinated ligands. For example, the P1–Rh–P2 angle of 96.76 (8)° is the largest in the basal plane and undoubtedly results from a minimization of the nonbonded contacts between ethyl groups of the phosphine ligands. Also the nonbonded interaction of the α-methylene protons of the acyl ligand with the π system of the mnt ligand leads to the apical bond angle distortions such that the average acyl–Rh–P and acyl–Rh–S bond angles are 92.20 (21) and 101.40 (20)°, respectively. However, these distortions preserve the essential C_s symmetry of the complex.

Conclusions.

The rhodium(I) carbonyl dithiolate $[Rh(CO)(PEt_3)(mnt)]^-$ is easily generated in situ by the addition of PEt_3 to solutions of $[Rh(CO)_2(mnt)]^-$, and the complex reacts readily with a variety of alkyl iodides and bromides to form acyl complexes which are isolated as neutral bis(phosphine) species of formula $Rh(COR)(PEt_3)_2(mnt)$. The structure of these neutral Rh(III)–acyl complexes has been shown to be square pyramidal with the acyl group in the unique apical position. Undoubtedly, oxidative addition and migratory insertion are involved in the formation of the acyl complexes, and we believe both of these steps precede incorporation of the second phosphine which substitutes for the halide ion of the starting substrate. The starting rhodium(I) dithiolate is also reactive enough to form in strong acid an isolable hydride or in the presence of ethylene a propionyl compound through the sequence of olefin coordination, insertion into an M–H bond, and migratory insertion of CO.

Acknowledgment. We wish to acknowledge the support of the National Science Foundation (Grant CHE 76-17440) for partial support of this work and Matthey Bishop, Inc., for a generous loan of rhodium salts. We also thank Dr. Dan E. Hendriksen for the spectrophotometric titration, Dr. E. C. Baker and Mr. C. P. Kubiak for help with the X-ray determination, and Professor R. Hoffmann for a preprint of his paper.

Registry No. $[AsPh_4][Rh(CO)(PEt_3)(mnt)]$, 69501-72-0; $Rh(COMe)(PEt_3)_2(mnt)$, 65595-40-6; $Rh(COEt)(PEt_3)_2(mnt)$, 65595-41-7; $Rh(CO\text{-}n\text{-}Pr)(PEt_3)_2(mnt)$, 65595-42-8; $Rh(CO\text{-}n\text{-}Bu)(PEt_3)_2(mnt)$, 65595-43-9; $Rh(CO\text{-}n\text{-}(CH_2)_9CH_3)(PEt_3)_2(mnt)$, 65595-44-0; $Rh[COCH_2CH(CH_3)_2](PEt_3)_2(mnt)$, 69501-73-1; $Rh[COCH(CH_3)_2](PEt_3)_2(mnt)$, 69501-74-2; $Rh(COC_3H_5)(PEt_3)_2(mnt)$, 65585-71-9; $Rh(COCH_2Ph)(PEt_3)_2(mnt)$, 65585-70-8; $Rh(COCH_2CCH)(PEt_3)_2(mnt)$, 69501-75-3; $Rh(H)(CO)(PEt_3)_2(mnt)$, 65652-54-2; $(PPh_3CH_3)[Rh(CO)(PEt_3)(mnt)]$, 69501-76-4; $[(n\text{-}Bu)_4N][Rh(CO)_2(mnt)]$, 30845-95-5; $[AsPh_4][Rh(CO)_2(mnt)]$, 63159-10-4; $[PPh_4][Rh(CO)_2(mnt)]$, 63159-11-5; MeI, 74-88-4; EtI, 75-03-6; *n*-PrI, 107-08-4; *n*-BuI, 542-69-8; $n\text{-}C_{10}H_{21}I$, 2050-77-3; *i*-BuI, 513-38-2; *i*-PrI, 75-30-9; allyl bromide, 106-95-6; benzyl bromide, 100-39-0; propargyl bromide, 106-96-7; *n*-BuBr, 109-65-9; *n*-PrBr, 106-94-5; EtBr, 74-96-4; allyl chloride, 107-05-1.

Supplementary Material Available: A listing of structure factor amplitudes (17 pages). Ordering information is given on any current masthead page.

References and Notes

(1) For example: (a) R. F. Heck, *J. Am. Chem. Soc.*, **86**, 2796 (1964); (b) M. C. Baird, J. T. Mague, J. A. Osborn, and G. Wilkinson, *J. Chem. Soc. A*, 1347 (1967); (c) A. J. Deeming and B. L. Shaw, *ibid.*, 597 (1969); (d) I. C. Douek and G. Wilkinson, *ibid.*, 2604 (1969); (e) A. J. Oliver and W. A. G. Graham, *Inorg. Chem.*, **9**, 243 (1970); (f) H. D. Empsall, E. M. Hyde, C. E. Jones, and B. L. Shaw, *J. Chem. Soc., Dalton Trans.*, 1980 (1974).
(2) A. J. Hart-Davis and W. A. G. Graham, *Inorg. Chem.*, **9**, 2658 (1970).
(3) C.-H. Cheng, B. D. Spivack, and R. Eisenberg, *J. Am. Chem. Soc.*, **99**, 3003 (1977).
(4) C.-H. Cheng, D. E. Hendriksen, and R. Eisenberg, *J. Organomet. Chem.*, **142**, C65 (1977).
(5) "International Tables for X-Ray Crystallography", Vol. 1, Kynoch Press, Birmingham, England, 1960, p 150.
(6) The programs for refinement of lattice constants and automated operation of the diffractometer are those of Busing and Levy as modified by Picker Corp.
(7) S. Z. Goldberg, C. Kubiak, C. D. Meyer, and R. Eisenberg, *Inorg. Chem.*, **14**, 1650 (1975).
(8) P. W. R. Corfield, R. J. Doedens, and J. A. Ibers, *Inorg. Chem.*, **6**, 197 (1967).
(9) Data reduction was performed with an extensively modified version of Raymond's URFACS. In addition, local versions of the following were used: Ibers' NUCLS, a group least-squares version of the Busing–Levy ORFLS program; Zalkin's FORDAP Fourier program; ORFFE, a function and error program by Busing, Martin, and Levy; Johnson's ORTEP thermal ellipsoid plotting program. All computations were carried out on an IBM 360/65 computer.
(10) D. T. Cromer and B. Mann, *Acta Crystallogr., Sect. A*, **24**, 321 (1968).
(11) D. T. Cromer and D. Lieberman, *J. Chem. Phys.*, **53**, 1891 (1970).
(12) R. F. Stewart, E. R. Davidson, and W. T. Simpson, *J. Chem. Phys.*, **42**, 3175 (1965).
(13) Supplementary material.
(14) N. G. Connelly and J. A. McCleverty, *J. Chem. Soc. A*, 1621 (1970).
(15) The previously reported value in ref 4 is wrong.
(16) J. Chatt, N. P. Johnson, and B. L. Shaw, *J. Chem. Soc.*, 1625 (1964).
(17) (a) D. L. Egglestone, M. C. Baird, C. J. L. Lock, and G. Turner, *J. Chem. Soc., Dalton Trans.*, 1576 (1977); (b) K. S. Y. Lau, Y. Becker, F. Huang, N. Baenziger, and J. K. Stille, *J. Am. Chem. Soc.*, **99**, 5664 (1977).
(18) H. Berke and R. Hoffmann, *J. Am. Chem. Soc.*, in press.
(19) G. W. Adamson, J. J. Daly, and D. Forster, *J. Organomet. Chem.*, **71**, C17 (1974).
(20) J. P. Collman, P. A. Christian, S. Current, P. Denisevich, T. R. Halbert, E. R. Schmittou, and K. O. Hodgson, *Inorg. Chem.*, **15**, 223 (1976), and references therein.
(21) R. J. Hoare and O. S. Mills, *J. Chem. Soc., Dalton Trans.*, 2138 (1972).
(22) J. A. Evans, D. R. Russell, A. Bright, and B. L. Shaw, *Chem. Commun.* 841 (1971).
(23) P. G. H. Troughton and A. C. Skapski, *Chem. Commun.*, 575 (1968); 666 (1969).
(24) M. R. Churchill and K.-N. Chen, *Inorg. Chem.*, **15**, 788 (1976).
(25) R. Beckett and B. F. Hoskins, *Inorg. Nucl. Chem. Lett.*, **8**, 683 (1972); sacsac = dithioacetylacetonate.
(26) R. Richter, J. Kaiser, J. Sieler, and L. Kutschabsky, *Acta Crystallogr., Sect. B*, **31**, 1642 (1975).
(27) B. Cetinkaya, M. F. Lappert, G. M. McLaughlin, and K. Turner, *J. Chem. Soc., Dalton Trans.*, 1591 (1974).